Computer Methods in Biomechanics and Biomedical Engineering,
Vol. 10, No. 2, April 2007, 129–136

Taylor & Francis
Taylor & Francis Group

Concentration wave of a solute in an artery: the influence of curvature

GIUSEPPE PONTRELLI†* and AMABILE TATONE‡¶

†Istituto per le Applicazioni del Calcolo-CNR, Viale del Policlinico, 137-00161 Roma, Italy
‡DISAT, Facoltà di Ingegneria, Università dell'Aquila, Monteluco di Roio (AQ), 67040 Aquila, Italy

(Received 19 September 2006; in final form 28 September 2006)

Mass transport and diffusion phenomena in the arterial lumen are studied through a mathematical model. Blood flow is described by the unsteady Navier–Stokes equation and solute dynamics by an advection–diffusion equation, the convective field being provided by the fluid velocity. A linearization procedure over the steady state solution is carried out and an asymptotic analysis is used to study the effect of a small curvature with respect to the straight tube.

Analytical and numerical solutions are found: the results show the characteristics of the long wave propagation and the role played by the geometry on the solute distribution and demonstrate the strong influence of curvature induced by the fluid dynamics.

Keywords: Mass transport; Diffusion-advection equation; Vascular flow; Curved arteries; Perturbation methods

1. Introduction

Extensive studies of the arterial mass transport processes become more and more important because of their relationship with atherogenesis. Actually, it is recognized that changes in wall permeability, related to an increased accumulation of materials on the subendothelial intima, are associated with early atherosclerotic lesions (Friedman *et al.* 1987).

Mathematical modelling and computer simulations of arterial fluid–wall mechanics and of transport process offer several advantages compared with experimental methods. They enable to quantify variables of physiological interest, such as wall shear stress or mass flux, otherwise inaccessible or difficult to obtain with measurements. Therefore, computational fluid dynamics reveals an appropriate tool for investigating vascular flow and physiological related processes such as diffusion and convection of a substance in the arterial lumen and through the vascular wall.

A number of models coupling 3D flow and solute dynamics have been developed in recent years (Rappitsch *et al.* 1997, Karner *et al.* 2000, Prosi *et al.* 2004). They are defined in a finite arterial segment, where an inflow distribution is provided. Some of them consider also absorption and exchange through the vascular tissues (Prosi *et al.* 2004). All these models provide the local concentration pattern and are useful to understand the relationship between the local flow pattern, the nourishing of arterial tissues and possible pathologies derived when such a process is altered (Quarteroni *et al.* 2002).

It is believed that fluid mechanical factors, such as flow separation, recirculation and wall shear stress, play a key role in the transport and in the accumulation of cholesterol and other solutes on the wall and thus in changing the permeability of the endothelial cells. However, due to the highly complex nature of the system, the precise response of the vessel to the wall shear stress is not yet understood. These phenomena tend to occur primarily in low shear rate regions and in sites of branching or bending, where flow axisymmetry is lost. In particular geometrical effects, such as curvature, will strongly affect the flow pattern and consequently the concentration of gases and other substances dissolved in the blood (Moore and Ethier 1997, Prosi *et al.* 2004). Moreover, mass transfer phenomena are intrinsically coupled with the hemodynamics which influences the wall permeability and fluid diffusivity (Stangeby and Ethier 2002).

The oscillating flow through an elastic thin-walled curved artery has been recently investigated, using an

*Corresponding author. Email: pontrelli@iac.rm.cnr.it
¶ Email: tatone@ing.univaq.it

Computer Methods in Biomechanics and Biomedical Engineering
ISSN 1025-5842 print/ISSN 1476-8259 online © 2007 Taylor & Francis
http://www.tandf.co.uk/journals
DOI: 10.1080/10255840601046048

asymptotic analysis under the assumption of small curvature (Pontrelli and Tatone 2005). In the present paper, a similar approach is used to model the mass transport and the diffusion process inside a straight or moderately curved artery. This is described by the advection–diffusion equation and a Robin-like interface condition is imposed at the permeable boundary to match internal and external fluxes and with the flow field preassigned. For most substances, such a process is highly convection dominated, due to a low diffusion coefficient (Moore and Ethier 1997). Being interested in propagative phenomena, the solute dynamics inside the vascular tissue is deemed a negligible phenomena and the so called *free-wall* model is used (Quarteroni *et al.* 2002). Induced by the periodicity of respiratory, hormonal and feeding acts, the concentration of a substance in blood is subject both to an oscillation in time and to a spatial variation along the vessel, sustained by the fluid motion. For example, the pulsatile insulin release in the blood stream is induced by the oscillation in glycolysis and generates a wave of period 5–10 min (Pedersen *et al.* 2005). In general, the wave period is strongly dependent of the solute considered. As a consequence, for any substance, we look for the propagation characteristics, in relation with the medium diffusivity and wall permeability properties.

The goal of this paper is to characterize the solute propagation in the blood flow and to provide the local distribution of concentration that can be influenced by geometrical factors, such as the curvature. The study, limited to small value of curvature, indicates the tendency and the strong sensitivity of the solution on the physical parameters. Translation and torsion effects where not included in the present work. Analysis and results are limited to small curvature and indicate a tendency and some numerical simulations show the dispersion curve and predict an asymmetric profile for concentration. This may reveal some correlation between flow pattern and process of altered absorption or anomalous accumulation of substances on the arterial wall.

The layout of this paper is as follows: in Section 2, the mathematical problem is stated as a convection–diffusion equation. A linearization process over a steady state solution is accomplished to split the concentration variable from the fluid dynamical field. A wave type solution is found for the unsteady component (Section 3) and a perturbation method is used to separate the dominant component in a straight tube from the part due to a possible small curvature (Section 4). Finally, in Section 5 some numerical experiments show the characteristics of the wave propagation in a straight and in a bended artery and the effect of geometrical factors on the solute distribution.

2. A mathematical model for solute dynamics

Different substances are dissolved in blood, transported through the stream and possibly exchanged through the arterial wall. For simplicity, the presence of one solute only is considered and its concentration denoted by c. Because of both diffusive and convective phenomena, c satisfies the following advection–diffusion equation (Bird *et al.* 1960, Caro *et al.* 1978, Rappitsch *et al.* 1997):

$$\frac{\partial c}{\partial t} + \mathbf{v}\cdot\nabla c - \nabla\cdot(\mu\nabla c) = 0 \tag{2.1}$$

with $\mathbf{v}$ the fluid velocity, $\mu > 0$ a diffusivity coefficient. A possible exchange of solute through the permeable wall is expressed by:

$$(\mu\nabla c)\cdot\mathbf{n} + \sigma c = \sigma c_{\text{ext}} \tag{2.2}$$

where $\sigma \geq 0$ is the wall permeability and c_{ext} is an external constant concentration (if the wall is impermeable, $\sigma = 0$). Strictly speaking, μ and σ should depend on the flow field and on the temperature but, for simplicity, let us assume them as constant. Any possible solute chemical reacting effect is also neglected.

A filtration flow through the porous layers of the arterial wall $c\cdot\mathbf{v}_{\text{filt}}$ may be present in equation (2.2), but its magnitude is negligible for dissolved gases and low molecular weight substances (Karner *et al.* 2000) and is not considered here.

Due to the small value of μ, for most substances the problem is highly convection dominated in large arteries. For $\mu \to 0$, the problem changes nature and tends to be purely hyperbolic (see Section 3). Note that the problem (2.1) and (2.2) is homogeneous when $c_{\text{ext}} = 0$ or when $\sigma = 0$ and admits ∞^1 solutions.

In principle, fluid and solute dynamics are coupled processes and influence reciprocally. However in this model, the solute is regarded as a passive scalar: it is simply advected by the blood flow in the lumen, neglecting any feedback effect on the fluid viscosity and density. As consequence, we split the flow problem from the solute dynamics: the fluid velocity $\mathbf{v}$ is computed beforehand and the problem (2.1) and (2.2) is subsequently solved.

Let us decompose the variables $\mathbf{v}$ and c as then sum of a steady part (denoted with a bar) and an unsteady component (indicated with a circumflex accent):

$$\mathbf{v} = \bar{\mathbf{v}} + \hat{\mathbf{v}} \qquad c = \bar{c} + \hat{c} \tag{2.3}$$

and let us assume the unsteady parts $\hat{\mathbf{v}}$ and $\hat{c}$ (and also $\nabla\hat{\mathbf{v}}$ and $\nabla\hat{c}$) are *small* enough with respect to the steady ones such that the nonlinear term $\mathbf{v}\cdot\nabla c$ in equation (2.1) can be linearized as:

$$(\bar{\mathbf{v}} + \hat{\mathbf{v}})\cdot(\nabla\bar{c} + \nabla\hat{c}) \approx \bar{\mathbf{v}}\cdot\nabla\bar{c} + \bar{\mathbf{v}}\cdot\nabla\hat{c} + \hat{\mathbf{v}}\cdot\nabla\bar{c} \tag{2.4}$$

neglecting the higher order terms. In other words, only small fluctuations of velocity and concentration over the steady solution are admitted.

It is straightforward to verify that any constant concentration:

$$\bar{c} = \begin{cases} c_{\text{ext}} & \text{if } \sigma \neq 0 \\ \text{const.} & \text{if } \sigma = 0 \end{cases} \tag{2.5}$$

satisfies the following steady boundary value problem:

$$\begin{aligned} &\bar{\mathbf{v}}\cdot\nabla\bar{c} - \mu\Delta\bar{c} = 0 \\ &\mu\nabla\bar{c}\cdot\mathbf{n} + \sigma\bar{c} = \sigma c_{\text{ext}} \quad \text{at the wall} \end{aligned} \tag{2.6}$$

This corresponds to the fact that, for a time long enough, the solute pervades the whole tube and, finally, reaches a uniform concentration. Because no further hypothesis has been made, the steady solution turns out to be independent either of the domain geometry and of the velocity field.

3. Unsteady solution

By equations (2.4) and (2.6), the unsteady solution satisfies the following equation:

$$\frac{\partial\hat{c}}{\partial t} + \bar{\mathbf{v}}\cdot\nabla\hat{c} + \hat{\mathbf{v}}\cdot\nabla\bar{c} - \mu\Delta\hat{c} = 0 \tag{3.1}$$

with an homogeneous boundary condition at the wall:

$$\mu\nabla\hat{c}\cdot\mathbf{n} + \sigma\hat{c} = 0 \tag{3.2}$$

Because of equations (2.5), the homogeneous boundary value problem (3.1) and (3.2) depends only on the steady fluid velocity $\bar{\mathbf{v}}$ and is independent of the unsteady flow field $\hat{\mathbf{v}}$ and of the steady concentration part $\bar{c}$ (note that, being external concentration constant in time, c_{ext} affects only the steady solution).

Let us now fix a precise shape to solve the problem (3.1) and (3.2). Let us consider a tube having the form of a long† cylinder which may have a small degree of curvature, in the shape of a torus. This has a planar axis, a circular cross section of radius a and constant radius of curvature R (figure 1). The small deformation of the walls, which is demonstrated of much importance in vascular dynamics (Pontrelli and Tatone 2005), is irrelevant for the solute motion. For the following analysis, it is convenient to work out the equations in a toroidal coordinate system $\{r, \theta, \psi\}$ (see figure 1). The axial coordinate $z = R\theta$ is introduced to avoid degeneracy when $R \to \infty$ (straight tube).

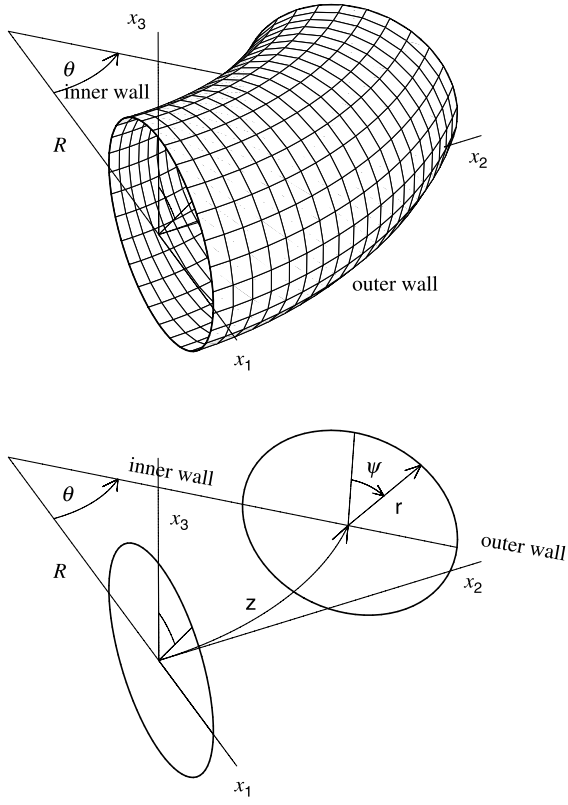

Figure 1. A portion of the curved tube between two cross sections (top). Toroidal coordinates (r, ψ, θ) and cartesian coordinates (x_1, x_2, x_3) (bottom).

3.1 Nondimensionalization

The problem is now rewritten in nondimensional form by the following substitutions:

$$\mathbf{x} \to \frac{\mathbf{x}}{a} \qquad t \to \frac{Vt}{a} \qquad \mathbf{v} \to \frac{\mathbf{v}}{V}$$

where $\mathbf{x}$ denotes the spatial coordinates and V is a characteristic velocity. Without loss of generality, the concentration is considered dimensionless.

Denoting by:

$$\begin{aligned} Pe &= \frac{aV}{\mu} \quad \text{(Péclet number)} \\ Sh &= \frac{a\sigma}{\mu} \quad \text{(Sherwood number)} \end{aligned} \tag{3.3}$$

two characteristic numbers (Sherwood number is a mass transfer coefficient), the governing equations (3.1) and (3.2) become:

$$\frac{\partial\hat{c}}{\partial t} + \bar{\mathbf{v}}\cdot\nabla\hat{c} - \frac{1}{Pe}\Delta\hat{c} = 0 \tag{3.4}$$

$$\nabla\hat{c}\cdot\mathbf{n} + Sh\,\hat{c} = 0 \tag{3.5}$$

†Here *long* means of length much larger than the radius. With such hypothesis the entry effects are disregarded.

3.2 Concentration wave

The physiological and metabolic functions of living beings are typically periodic and an intermittent release of substances (i.e. oxygen, hormones, nutrients, waste products) in the blood is carried out by several organs and glands (Johnson 2003). Digestive and respiratory acts are also based on a periodical time scale and, according to the species, period can range from seconds to hours. It is realistic to assume that, for each substance, there exists a pulsatile source of solute concentration that, advected by the fluid, propagates downstream. Being the blood flow essentially unidirectional, the unsteady component $\hat{c}$ has the form of an harmonic longitudinal travelling wave:

$$\hat{c} = \tilde{c}(r, \psi)\, \mathrm{e}^{\mathrm{i}(\omega t - kz)} \tag{3.6}$$

with ω a nondimensional circular frequency ($\omega \rightarrow \omega a/V$) and k the nondimensional wave number ($k \rightarrow ka$). Consequently, the nondimensional wave speed is $\omega/\mathrm{real}(k)$ and the nondimensional wavelength is $1/\mathrm{real}(k)$.

Concentration wave (3.6) has no direct relation with the wave of pressure and flow (included in the unsteady flow solution $\hat{\mathbf{v}}$, see equation (2.3) and foll.) generated by the heart beat and transmitted by the fluid thanks to the vessel distensibility. In physiological cases, ω is generally very low ($\omega \ll 1$).

3.3 The limit cases: $Pe \rightarrow 0$ and $Pe \rightarrow \infty$

For $Pe \rightarrow \infty$, the problem is of pure convection:

$$\frac{\partial \hat{c}}{\partial t} + \bar{\mathbf{v}}\cdot\nabla\hat{c} = 0 \qquad \nabla\hat{c}\cdot\mathbf{n} + Sh\,\hat{c} = 0 \tag{3.7}$$

and the wave solution has no physical meaning. Any initial distribution c_0 (satisfying the boundary conditions) is transported identically along the axial direction with velocity $\bar{\mathbf{v}}$ without any diffusion (this corresponds to a wave with $\omega = 0$ and $k = 0$).

For $Pe \rightarrow 0$, the problem becomes time independent:

$$\Delta\hat{c} = 0 \qquad \nabla\hat{c}\cdot\mathbf{n} + Sh\,\hat{c} = 0 \tag{3.8}$$

and admits as solution any constant $\hat{c}$ for $Sh = 0$ and $\hat{c} = 0$ for $Sh \neq 0$.

4. Perturbation solution

All arteries are affected by a small or moderate degree of curvature. A perturbation method is used to study the influence of a small curvature with respect to the straight case. As the curvature parameter $\varepsilon = a/R$ is assumed to be small ($\ll 1$), the solution in (3.6) is expanded as a power series of ε over an axisymmetric solution $c_0(r)$. By omitting the $\sim$ sign at the right hand side, we have:

$$\begin{aligned}\hat{c}(r, \psi) &= \hat{c}_0 + \varepsilon\hat{c}_1 + o(\varepsilon) \\ &= (c_0(r) + \varepsilon c_1(r, \psi))\, \mathrm{e}^{\mathrm{i}(\omega t - kz)} + o(\varepsilon)\end{aligned} \tag{4.1}$$

The fluid steady velocity $\bar{\mathbf{v}}$ undergoes a similar expansion over $\bar{\mathbf{v}}_0$:

$$\bar{\mathbf{v}}(r, \psi) = \bar{\mathbf{v}}_0(r) + \varepsilon\bar{\mathbf{v}}_1(r, \psi) + o(\varepsilon) \tag{4.2}$$

where $\bar{\mathbf{v}}_0$ is the Poiseuille velocity and $\bar{\mathbf{v}}_1$ is the first order velocity for a moderately curved tube (Dean 1927). Therefore one has:

$$\begin{aligned}\bar{\mathbf{v}}\cdot\nabla\hat{c} &= (\bar{\mathbf{v}}_0 + \varepsilon\bar{\mathbf{v}}_1)\cdot(\nabla\hat{c}_0 + \varepsilon\nabla\hat{c}_1) \\ &= \bar{\mathbf{v}}_0\cdot\nabla\hat{c}_0 + \varepsilon(\bar{\mathbf{v}}_1\cdot\nabla\hat{c}_0 + \bar{\mathbf{v}}_0\cdot\nabla\hat{c}_1) + o(\varepsilon)\end{aligned} \tag{4.3}$$

Expansions (4.1)–(4.3) are substituted in equations (3.4) and (3.5) and terms of the same power of ε, up to the first order, are equated.

4.1 0-th order solution

The concentration in a straight tube is governed by the following linear equation:

$$\frac{\partial\hat{c}_0}{\partial t} + \bar{\mathbf{v}}_0\cdot\nabla\hat{c}_0 - \frac{1}{Pe}\Delta\hat{c}_0 = 0 \tag{4.4}$$

By substituting the wave form (4.1) and neglecting all terms containing k^2 on the assumption that wavelengths are large in the present application, we get‡:

$$\frac{\mathrm{d}^2 c_0}{\mathrm{d}r^2} + \frac{1}{r}\frac{\mathrm{d}c_0}{\mathrm{d}r} + \mathrm{i}(k_\mathrm{P}\bar{w}_0 - \omega_\mathrm{P})c_0 = 0 \tag{4.5}$$

where $\omega_\mathrm{P} = \omega Pe$ (*scaled frequency*), $k_\mathrm{P} = kPe$ (*scaled wavenumber*) and

$$\bar{w}_0(r) = 1 - r^2$$

is the Poiseuille axial velocity profile, nondimensionalized by scaling with V.

The boundary conditions associated with the equation (4.5) are:

$$\frac{\mathrm{d}c_0}{\mathrm{d}r} = 0 \qquad \text{at } r = 0 \quad \text{(symmetry condition)} \tag{4.6}$$

$$\frac{\mathrm{d}c_0}{\mathrm{d}r} + Sh\,c_0 = 0 \qquad \text{at } r = 1 \tag{4.7}$$

For a given frequency ω_P, the Sturm–Liouville eigenvalue problem (4.5)–(4.7) is solved to obtain the wave number k_P which corresponds to an admissible c-wave solution in a straight tube. Consequently, a ∞†

‡$\omega = \frac{a^2\omega}{\mu}$ is a nondimensional parameter corresponding to the *Stokes number* (or to the square of *Womersley number*) for solute dynamics, with the fluid viscosity replaced by μ.

family of eigenfunctions c_0 relative to the couple (ω_P, k_P) is found.

Setting $G = (ik_P)^{1/2}$ and

$$H = \frac{(ik_P)^{1/2}}{4}\left(1 - \frac{\omega_P}{k_P}\right),$$

with the variable transformation¶

$$s = Gr^2 \qquad h(s) = 4ik_P r c_0(r) \tag{4.8}$$

equation (4.5) is rewritten as the Whittaker equation:

$$h''(s) + \left(\frac{1}{4s^2} - \frac{1}{4} + \frac{H}{s}\right)h(s) = 0 \tag{4.9}$$

which admits as solution a linear combination of confluent hypergeometric and generalized Laguerre functions (Abramowitz and Stegun 1972). By coming back through the inverse transformation of equation (4.8), we obtain the general integral of equation (4.5) written in terms of two constants A and B:

$$c_0(r) = \exp\left(-\frac{G}{2}r^2\right) \times \left[A\mathcal{L}\left(H - \frac{1}{2}, Gr^2\right) + B\mathcal{U}\left(\frac{1}{2} - H, 1, Gr^2\right)\right]r \tag{4.10}$$

with $\mathcal{L}$ the Laguerre function and $\mathcal{U}$ the Tricomi confluent hypergeometric function with complex argument.

A boundedness condition at $r = 0$ implies $B = 0$ and through the boundary condition (4.7), we obtain the frequency equation:

$$(\sqrt{k_P} + i^{3/2}Sh)\mathcal{L}\left(H - \frac{1}{2}, G\right) + 2\sqrt{k_P}\mathcal{L}_g\left(H - \frac{3}{2}, 1, G\right) = 0 \tag{4.11}$$

where $\mathcal{L}_g$ is the generalized Laguerre function. It gives the set of wavenumbers k_P correspondent to a given frequency ω_P. Finally, replacing them in equation (4.10), one has:

$$c_0(r) = A\exp\left(-\frac{(ik_P)^{1/2}}{2}r^2\right)\mathcal{L}\left(\frac{(ik_P)^{1/2}}{4}\left(1 - \frac{\omega_P}{k_P}\right) - \frac{1}{2}, \left(ik_P\right)^{1/2}r^2\right)r \tag{4.12}$$

The constant A can be expressed in terms of *mass per unit length*:

$$Q := \int_0^1 c_0(r) r \, dr \tag{4.13}$$

4.2 1st order solution

The correction due to a small curvature is described by the first order linear problem:

$$\frac{\partial \hat{c}_1}{\partial t} + \bar{\mathbf{v}}_0 \cdot \nabla \hat{c}_1 - \frac{1}{Pe}\Delta \hat{c}_1 = -\bar{\mathbf{v}}_1 \cdot \nabla \hat{c}_0 \tag{4.14}$$

i.e. in scalar form:

$$\frac{\partial^2 c_1}{\partial r^2} + \frac{1}{r}\frac{\partial c_1}{\partial r} + \frac{1}{r^2}\frac{\partial^2 c_1}{\partial \psi^2} + i(k_P \bar{w}_0 - \omega_P)c_1 = ik_P(r\bar{w}_0 - w_d)c_0 \sin\psi + (Pe\, u_d - 1)\frac{dc_0}{dr}\sin\psi \tag{4.15}$$

A solution of this nonhomogeneous equation is sought as:

$$c_1(r, \psi) = \check{c}_1(r)\sin\psi \tag{4.16}$$

Substitution of c_1 in equation (4.15) followed by $(\check{c}_1 \rightarrow c_1)$ gives:

$$\frac{\partial^2 c_1}{\partial r^2} + \frac{1}{r}\frac{\partial c_1}{\partial r} - \frac{c_1}{r^2} + i(k_P \bar{w}_0 - \omega_P)c_1 = ik_P(r\bar{w}_0 - w_d)c_0 + (Pe\, u_d - 1)\frac{dc_0}{dr} \tag{4.17}$$

together with the boundary conditions:

$$c_1 = 0 \qquad \text{at } r = 0 \tag{4.18}$$

$$\frac{dc_1}{dr} + Sh\, c_1 = 0 \qquad \text{at } r = 1 \tag{4.19}$$

where u_d and w_d are respectively the nondimensional radial and the axial component of the steady flow in a curved tube (Dean 1927):

$$u_d(r) = \frac{Re(1 - r^2)^2(4 - r^2)}{288}$$

$$w_d(r) = -\frac{3r(1 - r^2)}{4} + \frac{Re^2 r}{1152} \times \left[4(1 - r^2) - 3(1 - r^4) + (1 - r^6) - \frac{1 - r^8}{10}\right]$$

being $Re = aV/\nu$ the Reynolds number (with ν the fluid kinematic viscosity). Due to the antisymmetry of the first order solution c_1 (see equation (4.16)), the overall mass flux conservation of $c_0 + \varepsilon c_1$ in the half-section $(r, \psi) \in [0, 1] \times [-\pi/2, \pi/2]$ is guaranteed.

Note that the Péclet number appears at the right hand side of equation (4.17) as coefficient of u_d. The solution turns out to be strongly dependent on it, because it magnifies the role of secondary flow. Such effect exists as long as a transverse flow (u_d), induced by the curvature, is present and grows with Pe.

¶The problem was solved with the aid of the symbolic computing tool Mathematica®.

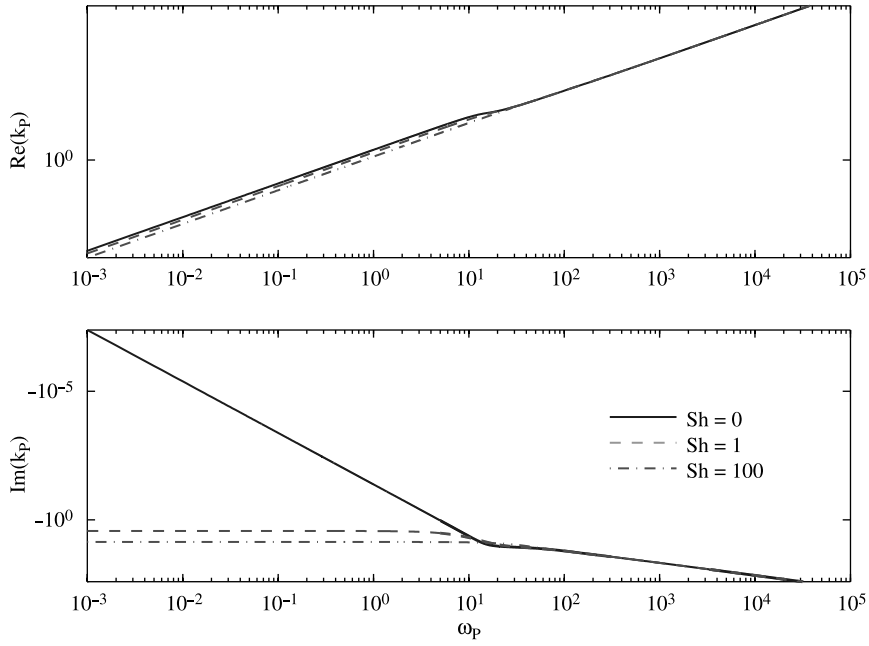

Figure 2. k vs. ω_P in loglog scale for three Sherwood numbers. For $\omega_P > 10$ the relation is almost linear irrespective of Sh.

5. Numerical results and discussion

The frequency equation (4.11) is solved numerically with a Newton type method by searching the complex roots k_P corresponding to a given ω_P. Owing to the large wavelength, only the smallest root is selected. Since we are interested in computing the solution for a set of frequencies and the problem being sensitive to the initial guess, a chain of continuation steps along the path $(\omega_P, c_0(\cdot, \omega_P))$ is initiated from $(0, c_0(\cdot, 0))$. At each step, the solution just obtained for ω_P is used as initial guess for solving the same problem with a subsequent close value $\omega_P + \Delta\omega_P$ (*continuation process*). Results show that both wavelength and attenuation reduce with increasing ω_P (figure 2) and the effect of wall permeability is present only for small frequencies.

The curve connecting the pairs $(\omega, (\omega/\text{real}(k_P))$ for $\omega_P \in [10^{-3}, 10^5]$ is shown in figure 3 (dispersion curve). It turns out that the wave speed tends to the asymptotic value 1 (independently of Sh), for relatively large values of the frequency. On the other hand, at very small frequencies the wave speed is rapidly decreasing tending to a finite limit as $\omega_P \to 0$. Such limit is $1/2$ for $Sh = 0$ and increases with Sh (figure 3). A critical frequency separates two regimes for each value of Sh: a layer where the velocity undergoes a sudden raise and a larger range where the velocity stays almost constant.

The exact solution c_0 of the boundary value problem (4.5)–(4.7) is given by equation (4.12) and normalized through equation (4.13). The boundary value problem (4.17)–(4.19) is then solved numerically with a collocation method using a cubic spline approximating function (Pryce 1993). The second order differential problem is firstly reformulated as a system of two first order ODE's. By means of an iterative procedure, the mesh is adapted in order to control the size of the residue and an initial guess is given by a quadratic polynomial satisfying the boundary conditions (Ascher *et al.* 1988). The method is fourth order accuracy and the algorithm is implemented through the routine bvp4c of MATLAB. Since it uses a closed integration formula, a simple recipe to avoid the singularity of the BVP (4.17) at 0 has been devised. The endpoint 0 has been replaced with $\delta = 10^{-5}$ and the BVP solved in $[\delta, 1]$ with a boundary condition in δ matching an extrapolated value.

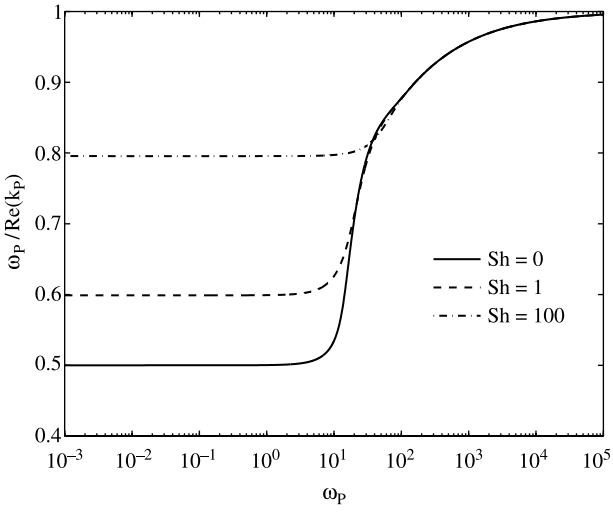

Figure 3. Dispersion curves for three Sherwood numbers. The wave speed tends to the same asymptotic value for relatively high frequencies and exhibits a variation with Sh only at very low frequencies. In a range of typical frequency ($10 \leq \omega_P \leq 100$), the speed undergoes a sudden raising.

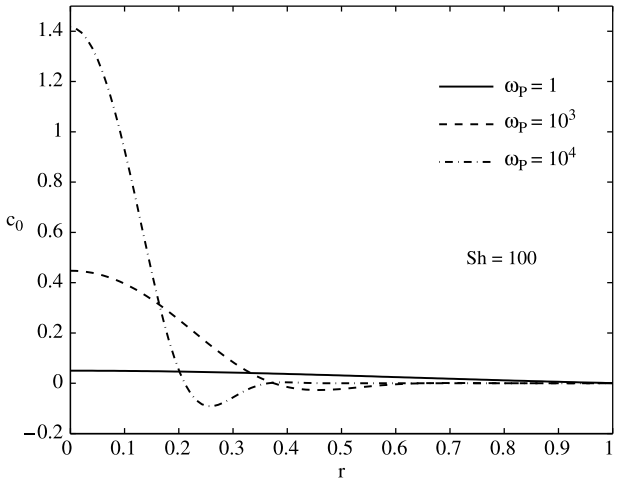

Figure 4. Concentration profiles along the horizontal half-diameter ($\psi = \pi/2$) of the cross section $z = 0$ at $t = 0$, for three values of ω_P. Differences with *Sh* are shown less pronounced and a core flux is evident at higher frequencies.

Once the analytical 0-th order solution is evaluated and the 1-st order problem solved numerically, the full wave solution is reassembled (see equations (2.3), (3.6) and (4.1)) as:

$$c = \bar{c} + \tilde{c}\,\mathrm{e}^{\mathrm{i}(\omega t - kz)} = \bar{c} + (c_0 + \varepsilon c_1 \sin\psi)\,\mathrm{e}^{\mathrm{i}(\omega t - kz)}$$

An harmonic form of the previous expression is:

$$c = \bar{c} + [\mathrm{real}(\tilde{c})\cos(\omega t - \mathrm{real}(k)z) - \mathrm{imag}(\tilde{c})\sin(\omega t - \mathrm{real}(k)z)]\,\mathrm{e}^{\mathrm{imag}(k)z} \tag{5.1}$$

or equivalently:

$$\chi = \bar{c} + |\tilde{c}|\cos\big(\omega t - \mathrm{real}(k)z + \phi\big)\mathrm{e}^{\mathrm{imag}(k)z} \quad \text{with} \quad \phi = \arg(\tilde{c}) \tag{5.2}$$

The physical problem depends on a number of parameters, each of them may vary in a quite wide range and there is a variety of different limiting cases. In the present work, we will focus the attention on the influence of the solution c on the diffusivity—parametrized by *Pe*—and on the wall permeability—parametrized by *Sh* (see equation (3.3)). These two parameters are varied in a convenient interval to describe a number of substances dissolved in blood and different medium properties.

Other parameters are fixed as:

$$a = 0.5\,\mathrm{cm} \quad \nu = 0.04\,\mathrm{poise} \quad V = 24\,\mathrm{cm\,s^{-1}} \quad Q = 0.01$$

giving $Re = 300$. A cross section of a curved tube with the inner wall at the left side is considered (figure 1).

Concentration amplitudes c_0 for three typical values of ω_P, with $Sh = 100$, are shown in figure 4. Approximately, flat concentration profiles at low ω_P, are replaced by more oscillating fronts, with a possible undershooting, at higher ω_P. At relatively higher ω_P, the concentration flux occurs in the core of the vessel and is independent of *Sh*. A moderate dependence of c on the wall permeability *Sh* exists at low scaled frequencies.

The influence of curvature is small at low *Pe*, but becomes relevant at higher *Pe*, with a more pronounced oscillating profile (figure 5). At the high Péclet numbers under consideration ($\approx 10^5$), a noticeable difference with

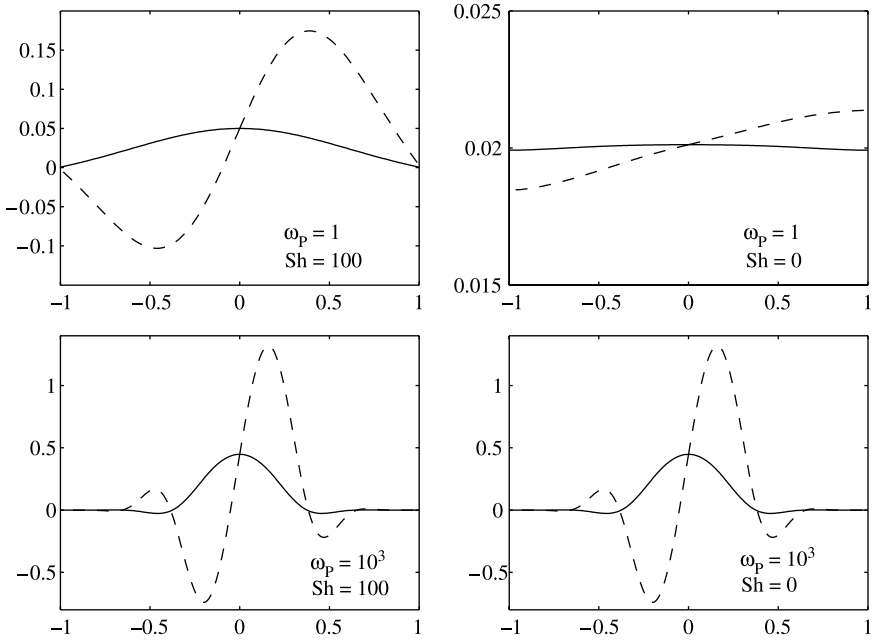

Figure 5. Concentration profiles along the horizontal diameter ($\psi = \pm\pi/2$) of the cross section $z = 0$ at $t = 0$ for $Pe = 10^5$ (inner wall on the left, outer wall on the right). Plots highlight the combined effects of the wall permeability *Sh* (left–right) and of the wave frequency ω_P (top–bottom) in the case of a straight tube (continuous line) and of a slightly curved tube with $\varepsilon = 10^{-4}$ (dashed line). For such value of *Pe*, the solution is extremely sensitive to the curvature and at low frequency, even to *Sh*.

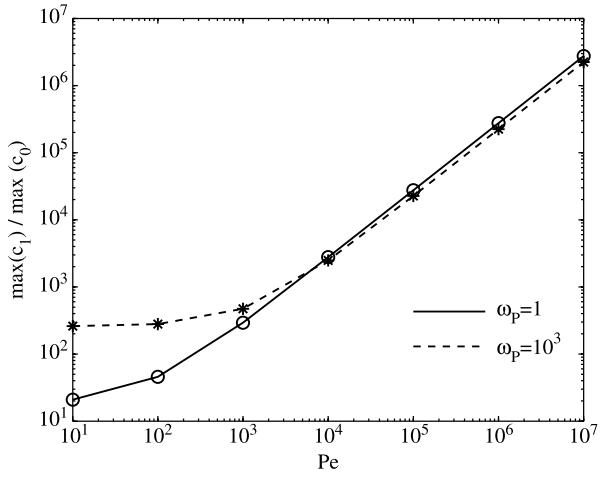

Figure 6. Ratio of the 1-st order solution over the 0-th order solution vs. the Péclet number at the cross section $z = 0$ and time $t = 0$ for two different ω_P ($Sh = 100$). Such ratio raises linearly for high Pe and provides an estimate of influence and sensitivity of the solution on the curvature.

respect to a straight tube appears even for a curvature ratio small as $\varepsilon = 10^{-4}$. The first order solution c_1 is of few orders of magnitude higher than c_0 and their ratio grows with Pe (figure 6). A significant result is the skewness of the c profiles: the maximum peak of concentration flux is shifted towards the outer bend and increases in magnitude (figure 5). Such first order correction due to the curvature is quantified as:

$$\Sigma(\varepsilon) = 2\varepsilon \int_0^{\pi/2} \sin\psi \, \mathrm{d}\psi \int_0^1 c_1(r) r \, \mathrm{d}r = 2\varepsilon \int_0^1 c_1(r) r \, \mathrm{d}r$$

The value of Σ results extremely sensitive to the value of Re and Pe.

6. Conclusions

Many phenomena, from biology to geophysics, from hydraulics to chemical engineering are described by convection and diffusion model problems, even at different time scales. In particular, transport of mass of particles passively advected by a tube flow has been studied by many investigators, for their considerable theoretical and practical interest.

Biomedical applications provided the source of inspiration for the present work: mass transport and diffusion phenomena inside a vessel and through the vascular wall are of great importance for physiological functions, such as oxygenation, nourishment of tissues and metabolic drainage processes. The problem is studied with respect to the characteristics of the long wave propagation in the arterial lumen, even in relation with a possible small curvature. Under this point of view, the description of mass transfer through the arterial wall has been disregarded. This approach is based on two simplifying hypotheses, which limit the applicability in realistic cases, but make the model a fundamental study and as idealized case, useful to understand the effects of the concurrent basic processes. The first is the linearization of the governing equations, justified by the small concentration amplitude and necessary to set up the theory of waves. A second limitation is the assumption of a fully developed flow: this is justified by long scale phenomena and has the advantage to avoid inlet/outer conditions and entrance effects.

The main result is a wall flux reduction at the inner wall of the curvature (figure 5). This is in correlation with clinical observations of atherosclerotic lesions at the inner wall of arterial bends. The wall permeability and compliance have been shown to have a low influence on the solute dynamics.

Acknowledgements

The authors wish to thank M. Prosi and P. Zunino for many fruitful discussions.

References

M. Abramowitz and I.A. Stegun (Eds.). “Handbook of mathematical functions”, Washington DC: National Bureau of Standards, 1972.

U. Ascher, R. Mattheij and R. Russell, “Numerical solution of boundary value problems for ordinary differential equations”, *Prentice Hall Series in Computational Mathematics*, Englewood Cliffs, NJ: Prentice Hall, Inc., 1988.

R.B. Bird, W.E. Stewart and E.N. Lightfoot, “Transport phenomena”, New York: John Wiley & Sons, 1960.

C.G. Caro, T.J. Pedley, R.C. Schroter and W.A. Seed, “The mechanics of the circulation”, Chapter 9, Oxford: Oxford University Press, 1978.

W.R. Dean, “Note on the motion of fluid in a curved pipe”, *Phil. Mag.*, 4, pp. 208–223, 1927.

M.H. Friedman, C.B. Bargeron, O.J. Deters, G.M. Hutchins and F.F. Mark, “Correlation between wall shear and intimal thickness at a coronary artery branch”, *Atherosclerosis*, 68, pp. 27–33, 1987.

T.D. Johnson, “Bayesian deconvolution analysis of pulsatile hormone concentration profile”, *Biometrics*, 59, pp. 650–660, 2003.

G. Karner, K. Perktold, H.P. Zehentner and M. Prosi, “Mass transport in large arteries and through the arterial wall”, in *Intra and Extracorporeal Cardiovascular Fluid Dynamics*, Adv. Fluid Mech. P. Verdonck and K. Perktold, Eds., Southampton, Boston: WIT press, 2000, pp. 209–247.

J.A. Moore and C.R. Ethier, “Oxygen mass transfer calculations in large arteries”, *J. Biomech. Eng.*, 119, pp. 469–475, 1997.

M.G. Pedersen, R. Bertram and A. Sherman, “Intra- and inter-islet synchronization of metabolically driven insulin secretion”, *Biophys. J. BioFAST*, doi:10.1529/biophysj.104.055681, April 15. 2005.

G. Pontrelli and A. Tatone, “Wave propagation in a fluid flowing through a curved thin-walled elastic tube”, *Eur. J. Appl. Mech. Fluids*, 25, pp. 987–1007, 2006.

M. Prosi, K. Perktold, Z. Ding and M.H. Friedman, “Influence of curvature dynamics on pulsatile coronary artery flow in a realistic bifurcation model”, *J. Biomech.*, 37, pp. 1767–1775, 2004.

J.D. Pryce, “Numerical solution of Sturm–Liouville problems”, *Monographs on Numerical Analysis*, Oxford, UK: Oxford University Press, 1993, p. 0.

A. Quarteroni, A. Veneziani and P. Zunino, “Mathematical and numerical modeling of solute dynamics in blood flow and arterial walls”, *SIAM. J. Num. Anal.*, 39(5), pp. 1488–1511, 2002.

G. Rappitsch, K. Perktold and E. Pernkopf, “Numerical modelling of shear-dependent mass transfer in large arteries”, *Int. J. Num. Meth. Fluids*, 25, pp. 847–857, 1997.

D.K. Stangeby and C.R. Ethier, “Computational analysis of coupled blood–wall arterial LDL transport”, *J. Biomech. Eng.*, 124, pp. 1–8, 2002.